Pure Spin Current Injection in Hydrogenated Graphene Structures

Reinaldo Zapata-Peña[1], Bernardo S. Mendoza[1], Anatoli I. Shkrebtii[2]

[1]Centro de Investigaciones en Óptica, León, Guanajuato 37150, México and

[2]University of Ontario, Institute of Technology, Oshawa, ON, L1H 7L7, Canada
(Dated: May 9, 2017)

Lorem ipsum dolor sit amet, consectetuer adipiscing elit. Etiam lobortis facilisis sem. Nullam nec mi et neque pharetra sollicitudin. Praesent imperdiet mi nec ante. Donec ullamcorper, felis non sodales commodo, lectus velit ultrices augue, a dignissim nibh lectus placerat pede. Vivamus nunc nunc, molestie ut, ultricies vel, semper in, velit. Ut porttitor. Praesent in sapien. Lorem ipsum dolor sit amet, consectetuer adipiscing elit. Duis fringilla tristique neque. Sed interdum libero ut metus. Pellentesque placerat. Nam rutrum augue a leo. Morbi sed elit sit amet ante lobortis sollicitudin. Praesent blandit blandit mauris. Praesent lectus tellus, aliquet aliquam, luctus a, egestas a, turpis. Mauris lacinia lorem sit amet ipsum. Nunc quis urna dictum turpis accumsan semper.

I. INTRODUCTION

Lorem ipsum dolor sit amet, consectetuer adipiscing elit. Etiam lobortis facilisis sem. Nullam nec mi et neque pharetra sollicitudin. Praesent imperdiet mi nec ante. Donec ullamcorper, felis non sodales commodo, lectus velit ultrices augue, a dignissim nibh lectus placerat pede. Vivamus nunc nunc, molestie ut, ultricies vel, semper in, velit. Ut porttitor. Praesent in sapien. Lorem ipsum dolor sit amet, consectetuer adipiscing elit. Duis fringilla tristique neque. Sed interdum libero ut metus. Pellentesque placerat. Nam rutrum augue a leo. Morbi sed elit sit amet ante lobortis sollicitudin. Praesent blandit blandit mauris. Praesent lectus tellus, aliquet aliquam, luctus a, egestas a, turpis. Mauris lacinia lorem sit amet ipsum. Nunc quis urna dictum turpis accumsan semper. Lorem ipsum dolor sit amet, consectetuer adipiscing elit. Etiam lobortis facilisis sem. Nullam nec mi et neque pharetra sollicitudin. Praesent imperdiet mi nec ante. Donec ullamcorper, felis non sodales commodo, lectus velit ultrices augue, a dignissim nibh lectus placerat pede. Vivamus nunc nunc, molestie ut, ultricies vel, semper in, velit. Ut porttitor. Praesent in sapien. Lorem ipsum dolor sit amet, consectetuer adipiscing elit. Duis fringilla tristique neque. Sed interdum libero ut metus. Pellentesque placerat. Nam rutrum augue a leo.
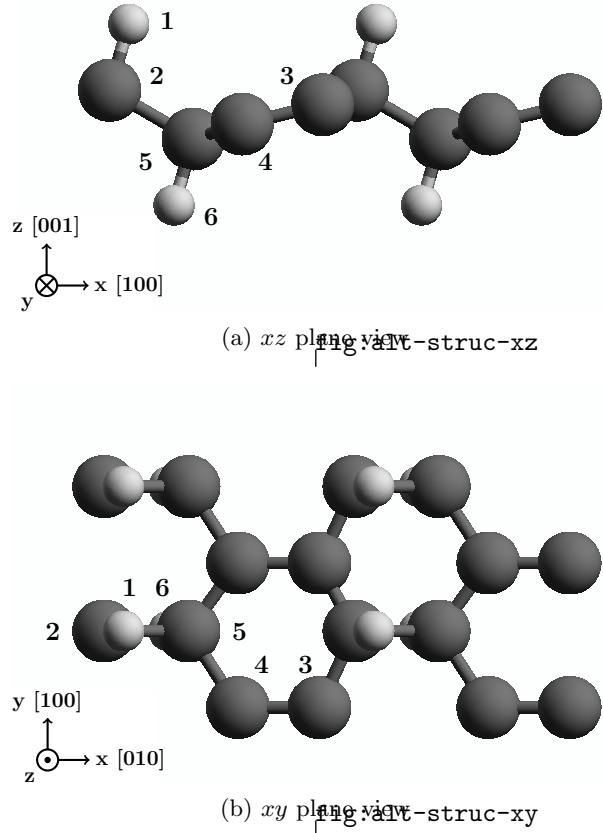

(a) xz plane view

(b) xy plane view

FIG. 1. Alt structure

Morbi sed elit sit amet ante lobortis sollicitudin. Praesent blandit blandit mauris. Praesent lec-

(a) xz plane view `fig:up-struc-xz`

(b) xy plane view `fig:up-struc-xy`

FIG. 2. Up structure `fig:up-struc`

tus tellus, aliquet aliquam, luctus a, egestas a, turpis. Mauris lacinia lorem sit amet ipsum. Nunc quis urna dictum turpis accumsan semper. Lorem ipsum dolor sit amet, consectetuer adipiscing elit. Etiam lobortis facilisis sem. Nullam nec mi et neque pharetra sollicitudin. Praesent imperdiet mi nec ante. Donec ullamcorper, felis non sodales commodo, lectus velit ultrices augue, a dignissim nibh lectus placerat pede. Vivamus nunc nunc, molestie ut, ultricies vel, sem-

per in, velit. Ut porttitor. Praesent in sapien. Lorem ipsum dolor sit amet, consectetuer adipiscing elit. Duis fringilla tristique neque. Sed interdum libero ut metus. Pellentesque placerat. Nam rutrum augue a leo. Morbi sed elit sit amet ante lobortis sollicitudin. Praesent blandit blandit mauris. Praesent lectus tellus, aliquet aliquam, luctus a, egestas a, turpis. Mauris lacinia lorem sit amet ipsum. Nunc quis urna dictum turpis accumsan semper.

Lorem ipsum dolor sit amet, consectetuer adipiscing elit. Etiam lobortis facilisis sem. Nullam nec mi et neque pharetra sollicitudin. Praesent imperdiet mi nec ante. Donec ullamcorper, felis non sodales commodo, lectus velit ultrices augue, a dignissim nibh lectus placerat pede. Vivamus nunc nunc, molestie ut, ultricies vel, semper in, velit. Ut porttitor. Praesent in sapien. Lorem ipsum dolor sit amet, consectetuer adipiscing elit. Duis fringilla tristique neque. Sed interdum libero ut metus. Pellentesque placerat. Nam rutrum augue a leo. Morbi sed elit sit amet ante lobortis sollicitudin. Praesent blandit blandit mauris. Praesent lectus tellus, aliquet aliquam, luctus a, egestas a, turpis. Mauris lacinia lorem sit amet ipsum. Nunc quis urna dictum turpis accumsan semper.

II. THEORY

`sec:theory`

A. Pure spin velocity

`sec:theory-pure_spin_current`

The spin density injection current $\dot{K}^{\mathrm{ab}}$ with speed along direction a and spin polarization along b is defined as

$$\dot{K} = \mu^{\mathrm{abcd}}(\omega) E^{\mathrm{c}}(\omega) E^{\mathrm{d}*}(\omega) \qquad \text{`eq:dotk`} \quad (1)$$

where

$$\mu^{\mathrm{abcd}}(\omega) = \frac{\pi e^2}{\hbar^2} \int \frac{d^3 K}{8\pi^3} \sideset{}{'}\sum_{vcc'} \mathrm{Re}\left[K^{\mathrm{ab}}_{cc'}(r^{\mathrm{c}}_{vc'} r^{\mathrm{d}}_{cv} + r^{\mathrm{d}}_{vc'} r^{\mathrm{c}}_{cv}) \right] \delta(\omega - \omega_{cv}) \qquad \text{`eq:mu`} \quad (2)$$

$$K^{\mathrm{ab}}_{mn} = \sum_{\ell} v^{\mathrm{a}}_{nl} S^{\mathrm{b}}_{lm} \qquad \qquad \text{`eq:velspi-matelem`} \quad (3)$$

is the corresponding spin density injection current pseudotensor. The $'$ in the sum means that

c and c' are quasi degenerate states and the sum only covers these states.

Now we define the spin velocity, $\mathcal{V}^{ab}$ as the speed at which the spin polarized in the b direc-

tion moves along the a direction when a normal incident beam reaches the xy plane with a polarization angle α. Then,

$$
\begin{aligned}
\mathcal{V}^{ab}(\omega) &= \frac{2}{\hbar} \frac{\mu^{abxx}(\omega)E^2(\omega)\cos^2(\alpha) + \mu^{abyy}(\omega)E^2(\omega)\sin^2(\alpha) + 2\mu^{abxy}(\omega)E^2(\omega)\cos(\alpha)\sin(\alpha)}{\xi^{xx}(\omega)E^2(\omega)\cos^2(\alpha) + \xi^{yy}(\omega)E^2(\omega)\sin^2(\alpha)}, \\
&= \frac{2}{\hbar} \frac{\mu^{abxx}(\omega)\cos^2(\alpha) + \mu^{abyy}(\omega)\sin^2(\alpha) + \mu^{abxy}(\omega)\sin(2\alpha)}{\xi^{xx}(\omega)\cos^2(\alpha) + \xi^{yy}(\omega)\sin^2(\alpha)}.
\end{aligned}
\tag{4}
$$

For an angle $\alpha = \frac{\pi}{4}$ this expression can be reduced to

$$
\mathcal{V}^{ab}(\omega) = \frac{2}{\hbar} \frac{\mu^{abxx}(\omega) + \mu^{abyy}(\omega) + 2\mu^{abxy}(\omega)}{\xi^{xx}(\omega) + \xi^{yy}(\omega)}.
\tag{5}
$$

B. Fixing spin

Considering that we have 2D structures we can fix the spin direction along the x, y, and z Cartesian coordinates and then define the magnitude of the spin velocity $|\mathcal{V}_{\sigma^b}|$ in a fixed angle γ_b as

$$
|\mathcal{V}_{\sigma^b}|(\omega) = \sqrt{(\mathcal{V}^{ax}(\omega))^2 + (\mathcal{V}^{ay}(\omega))^2},
\tag{6}
$$

$$
\gamma_b(\omega) = \tan^{-1}\left(\frac{\mathcal{V}^{ay}(\omega)}{\mathcal{V}^{ax}(\omega)}\right),
\tag{7}
$$

where the angle is measured in the counterclockwise direction from the positive x axis.

C. Fixing velocity.

In a similar way we can fix the velocity in the xy plane along x and y directions and define $|\mathcal{V}^a|$ as

$$
|\mathcal{V}^a|(\omega) = \sqrt{(\mathcal{V}^{ax}(\omega))^2 + (\mathcal{V}^{ay}(\omega))^2 + (\mathcal{V}^{az}(\omega))^2},
\tag{8}
$$

and the corresponding polar and azimuthal angles θ and φ as

$$
\theta_a(\omega) = \cos^{-1}\left(\frac{\mathcal{V}^{az}(\omega)}{|\mathcal{V}^a(\omega)|}\right), \quad 0 \le \theta \le \pi,
\tag{9}
$$

$$
\varphi_a(\omega) = \tan^{-1}\left(\frac{\mathcal{V}^{ay}(\omega)}{\mathcal{V}^{ax}(\omega)}\right), \quad 0 \le \varphi \le 2\pi.
\tag{10}
$$

D. Layer-by-layer analysis.

For a layered system we have that the total contribution of Eqns. (6) and (8) is given[1] by

$$
|\mathcal{V}_{\sigma^b}(\omega)| = \ell_{\text{eff}} \sum_{\ell=1}^{N_{\text{eff}}} |\mathcal{V}_{\sigma^b}(\ell|\omega)|,
\tag{11}
$$

$$
|\mathcal{V}^a(\omega)| = \ell_{\text{eff}} \sum_{\ell=1}^{N_{\text{eff}}} |\mathcal{V}^a(\ell|\omega)|.
\tag{12}
$$

III. RESULTS

We preset the results for $\mathcal{V}^{ab}$ for the $C_{16}H_8$-alt and $C_{16}H_8$-up structures being both noncentrosymmetric semi-infinite carbon systems with 50% hydrogenation in different arrangements. The *alt* system has alternating hydrogen atoms on the upper and bottom sides of the carbon sheet, while the *up* system has H only on the upper side. We take the hexagonal carbon lattice to be on the xy plane for both structures, and the carbon-hydrogen bonds on the perpendicular xz plane, as depicted in Figs. 1 and 2.

Layer	Atom	Position [Å]		
No.	type	x	y	z
1	H	-0.61516	-1.42140	1.47237
2	C	-0.61516	-1.73300	0.39631
3	C	0.61516	1.73300	0.15807
4	C	0.61516	0.42201	-0.15814
5	C	-0.61516	-0.37396	-0.39632
6	H	-0.61516	-0.68566	-1.47237

TABLE I. Unit cell of *alt* structure. Layer division, atom types and positions for the *alt* structure. The structure unit cell was divided in six layers corresponding each one to atoms in different z positions. The corresponding layer atom position is depicted in Fig. 1 with the corresponding number of layer. `tab:alt-unitcell`

Layer	Atom	Position [Å]		
No.	type	x	y	z
1	H	-0.61516	-1.77416	0.73196
1	H	0.61518	0.35514	0.73175
2	C	-0.61516	-1.77264	-0.49138
2	C	-0.61516	-0.35600	-0.72316
2	C	0.61516	0.35763	-0.49087

TABLE II. Unit cell of *up* structure. Layer division, atom types and positions for the *up* structure. The structure unit cell was divided in two layers corresponding to hydrogen and carbon atoms.The corresponding layer atom position is depicted in Fig. 2 with the corresponding number of layer. `tab:up-unitcell`

Using the ABINIT code[2] we calculated the self-consistent ground state and the Kohn-Sham states using density functional theory in the local density approximation (DFT-LDA) with a planewave basis. We used Hartwigsen-Goedecker-Hutter (HGH) relativistic separable dual-space Gaussian pseudopotentials[3] including the spin-orbit interaction needed to calculate $\mu^{\mathrm{abcd}}(\omega)$ (Eq. (2)) and $|\mathcal{V}^{\mathrm{a}}(\omega)|$ (Eq. (4)). It is known that using DFT-LDA to calculate the electronic structure of materials predict a different band gap than the obtained experimentally. A correction for the band gap energy value can be calculated by other *ab- initio* methods such as the GW approximation[4] but this is outside the scope of this paper. The convergence parameters for the calculations of our results corresponding
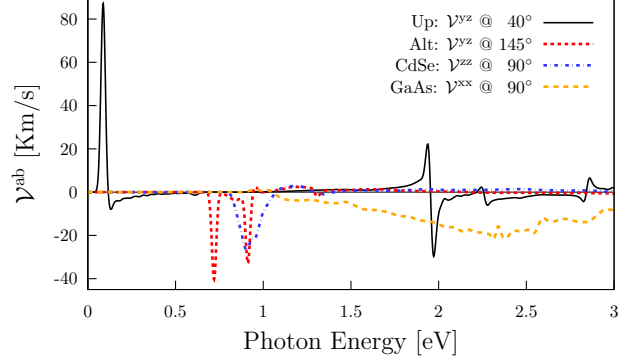

FIG. 3. Comparison of most intense responses of $\mathcal{V}^{\mathrm{ab}}$ for *alt*, *up*, CdSe, and GaAs structures and the corresponding polarization angles. `fig:vab-str-comp`

to the *alt* and *up* structures are cutoff energies of 65 Ha and 40 Ha, respectively. The energy eigenvalues and matrix elements were calculated using 14452 **k** points and 8452 **k** points in the irreducible Brillouin zone (IBZ) and present LDA energy band gaps of 0.72 eV and 0.088 eV, respectively for the *alt* and *up* structures.

A. Spin velocity

`sec:res-spin_velocity`

In figure 3 we present a comparison of the most intense responses resulting from evaluate the Eq. (4) for the *alt* and *up* 2D structures vs. CdSe and GaAs bulk structures. As we can see from this figure the most intense response corresponds to the *up* structure centered at 0.088 eV corresponding to the THz radiation and reaching a spin velocity of 87.16 Km/s. In the other hand, for an energy range from

Structure	Kind of	Pol.	Energy	$\mathcal{V}^{\mathrm{ab}}(\omega)$	
	system	Ang.	[eV]	ab	[Km/s]
up	2D	40	0.09	yz	87.16
			1.94	yz	22.22
			1.97	yz	-29.70
alt	2D	145	0.72	yz	-40.21
			0.91	yz	-32.89
CdSe	bulk	90	0.91	zz	-26.87
GaAs	bulk	90	2.31	xx	-21.62

TABLE III. Comparison of the reported maxima values of $\mathcal{V}^{\mathrm{ab}}$ for different structures and the corresponding polarization angle α and energy values. `tab:vab-str-comp`

0.66 eV to 3.0 eV, corresponding to energies of the Thz and visible radiation, all the four structures have contributions in the same order of magnitude. Starting with the 2D structures we have that the *up* structure has other two peaks centered at 1.94 eV and 1.97 eV reaching spin velocities of 22.2 Km/s and -29.7 Km/s, respectively, and the *alt* structure has two peaks centered at 0.72 eV and 0.91 eV reaching spin velocities of -40.2 Km/s and -32.9 Km/s, respectively. Then, for the bulk structures we have that the CdSe has only one intense response centered at 0.91 eV reaching a spin velocity of -26.9 Km/s, and the GaAs structure has a large and almost planar zone where the response is held reaching the maximum for an incoming beam of energy of 2.31 eV and reaching a spin velocity of -21.6 Km/s. In table III we present the comparison of this values for the 2D and bulk structures.

B. Fixing spin

Up structure

We first present two energy ranges for the *up* structure, the first for an incoming energy beam from 0.0 eV to 0.2 eV in the THz radiation range where the absolute maximum of the $|\mathcal{V}_{\sigma^z}|(\omega)$ response is obtained and the second for an energy range from 1.80 eV to 2.1 eV where two local maxima are found. In Fig. 4 we present the $|\mathcal{V}_{\sigma^z}|(\omega)$ spectra resulting from evaluate the Eq. (6) using different polarization angles α in the Eq. (4) for the *up* structure. In the figure we have that the onset of the response starts when the energy of the incoming beam is the same of the gap energy. From this figure we obtained that the zone where the maximum response is held corresponds to a energy range of the incident beam from 0.084 eV to 0.093 eV, corresponding to the THz radiation, and polarization angles α between 30° and 45°. Also two local maxima are held for same polarization angles but for an energy range of the incoming beam between 1.90 eV and 2.05 eV corresponding to the THz and visible radiation. In the top frames of Figs.5(a) and 5(b) we present in solid lines the result of evaluate $|\mathcal{V}_{\sigma^z}|(\omega)$, related to the left scale, fixing the energy of the incoming
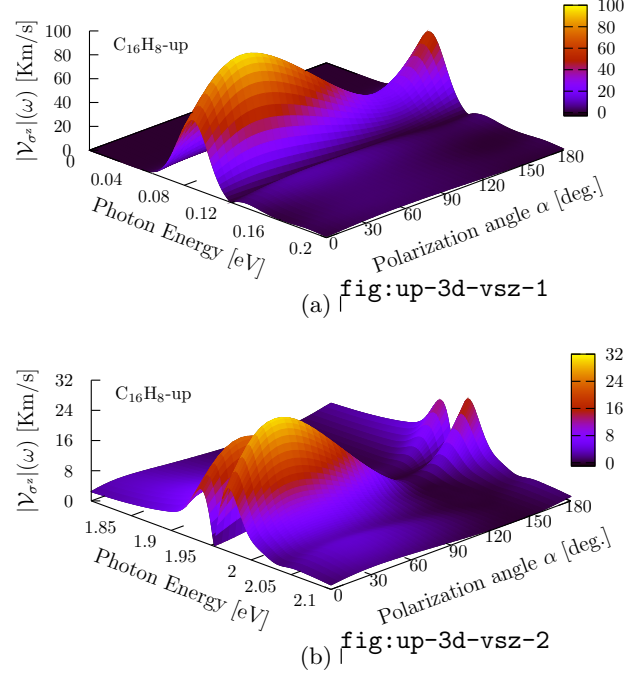

(a) fig:up-3d-vsz-1

(b) fig:up-3d-vsz-2

FIG. 4. $|\mathcal{V}_{\sigma^z}|(\omega)$, response vs. photon energy vs. polarization angle α for the *up* structure for two energy ranges. The absolute maxima is located for an energy range from 0.08 eV to 0.10 eV and the local maximum from 1.95 eV to 2.0 eV and both for polarization angles between 25° and 50°. fig:up-3d-vsz

beam to 0.088 eV and 0.912 eV, respectively, for which value the response is maximized for the *up* structure. In the same figures and frames we present in dashed lines, related to the right scale, the corresponding velocity angle $\gamma_z(\omega)$ obtained from the evaluation of Eq. (7), and in the bottom frames of those figures the corresponding components $\mathcal{V}^{xz}(\omega)$ and $\mathcal{V}^{yz}(\omega)$. Also we present two circled and square boxes indicating the values where the angles of the spin velocity are parallel and perpendicular and the the arrows are directed to the value of the response corresponding to those angles. From Figs. 5(a) and 4(a) we have that the absolute maximum response for the *up* structure is obtained for an incoming beam with energy of 0.088 eV and polarization angle $\alpha = 40°$ resulting in a value of $|\mathcal{V}_{\sigma^z}|(\omega) = 37.4$ Km/s coming from the contribution of the components $\mathcal{V}^{xz}(\omega) = 39.8$ Km/s and $\mathcal{V}^{yz}(\omega) = 87.2$ Km/s for the spin polarized in the z direction and having a velocity angle $\gamma_z(\omega) = 65°$ on the xy plane. In the same fig-
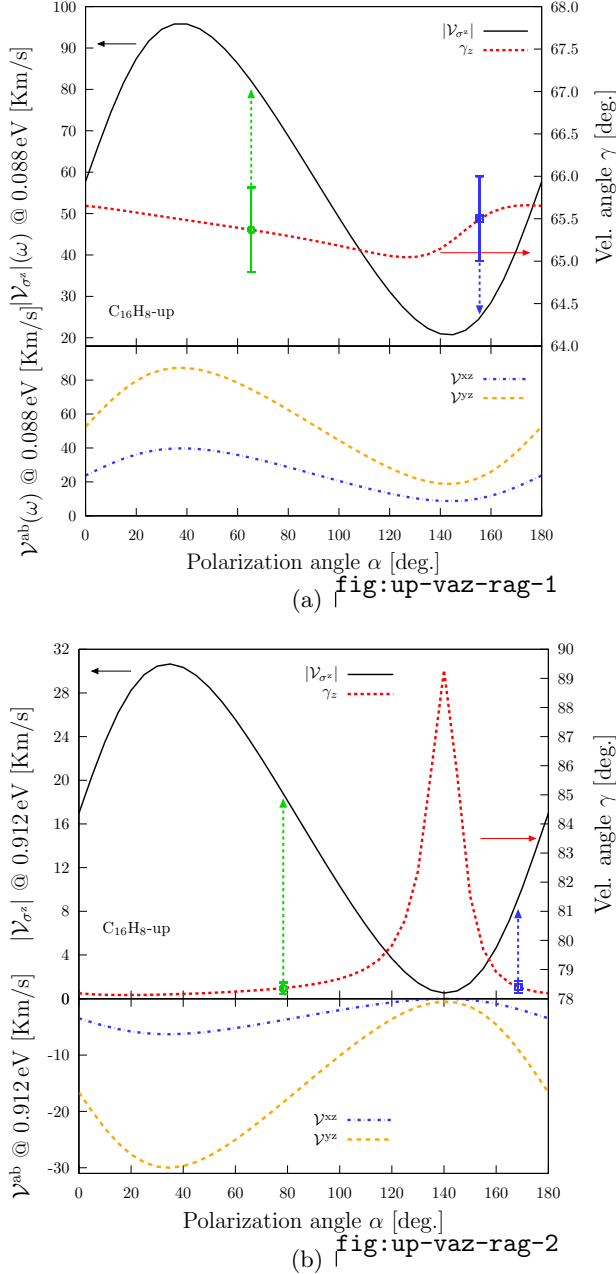
FIG. 5. Most intense response of $|\mathcal{V}_{\sigma^z}|(\omega)$ (top frames, right scale of figs (a) and (b)), the corresponding velocity angle $\gamma_z(\omega)$ (top frames, right scale), the collinear (circled box) and perpendicular (square box) angles, and the two components $\mathcal{V}^{xz}(\omega)$ and $\mathcal{V}^{yz}(\omega)$ (bottom frames) for the *up* structure fixing the energy to 0.088 eV.

`fig:up-vaz-rag`

ure the green circled box indicates the value for which the polarization angle α and the response direction angle $\gamma_z(\omega)$ are collinear being this angle 65.5° resulting in a value of the response of $|\mathcal{V}_{\sigma^z}|(\omega) = 82.3$ Km/s indicated by the upward

green arrow. Also the blue square box indicates the value for which the polarization angle and the response angle are perpendicular being $\alpha = 155.5°$ and $\gamma_x(\omega) = 65.5°$; for this angles the response has a value of $|\mathcal{V}_{\sigma^z}|(\omega) = 24.8$ Km/s indicated by the blue downward arrow. The green and blue error bars are fixed for a value of $\pm 0.5°$ and then, for this variation in the $\gamma_z(\omega)$ angle the complete range of α angle is included because this last is almost constant. Now from Figs. 5(b) and 4(b) we have that a local maxima of the response is obtained for an incoming beam with energy of 0.912 eV and same polarization angle $\alpha = 40°$ resulting in a value of $|\mathcal{V}_{\sigma^z}|(\omega) = 30.3$ Km/s directed in a velocity angle $\gamma_z(\omega) = 78°$ on the xy plane for the spin polarized in the z direction. Again the green circled box indicates the value for which the polarization angle α and the response direction angle $\gamma_z(\omega)$ are collinear being both 78.5° and having a response value of $|\mathcal{V}_{\sigma^z}|(\omega) = 23.5$ Km/s indicated with the green upward arrow. We found that for variations in the response angle of $\pm 2°$, indicated with the error bars, corresponds a range in the polarization angle of $0° \leq \alpha \leq 122°$ having then a large range for which the direction of the response is directed to this angle. The blue square box indicates the value for which the polarization angle and the response angle are perpendicular being $\alpha = 168.5°$ $\gamma_z(\omega) = 78.5°$ and having a response $|\mathcal{V}_{\sigma^z}|(\omega) = 9.0$ Km/s indicated with the blue upward arrow. Again, for variations in the response angle of $\pm 2°$, indicated with the error bars, corresponds a range in the polarization angle of $155° \leq \alpha \leq 180°$ having again a large range for which the direction of the response is held.

Alt structure

In Fig. 6 we present the $|\mathcal{V}_{\sigma^z}|(\omega)$ spectra resulting from evaluate again the Eq. (6) vs. the photon energy of the incident beam vs. the polarization angle α in Eq. (4) for the *alt* structure . In the figure we have that the onset of the response starts when the energy of the incoming beam is the same of the gap energy. From this figure we found that the zone where the absolute maximum response is held corresponds to a energy range from 0.90 eV to 0.93 eV, corresponding to the THz radiation, and polariza-
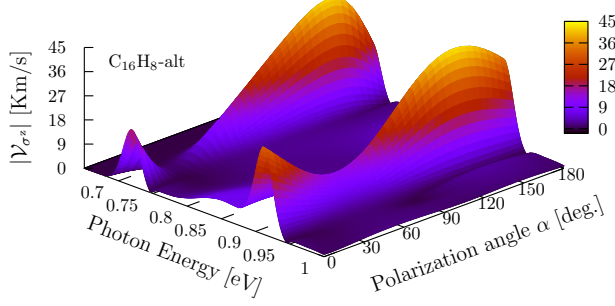
FIG. 6. $|\mathcal{V}_{\sigma^z}|(\omega)$, response vs. photon energy vs. polarization angle α for the *alt* structure. The absolute maximum is located for an energy range from $0.90\,\mathrm{eV}$ to $0.93\,\mathrm{eV}$ and for polarization angles between $120°$ and $150°$.
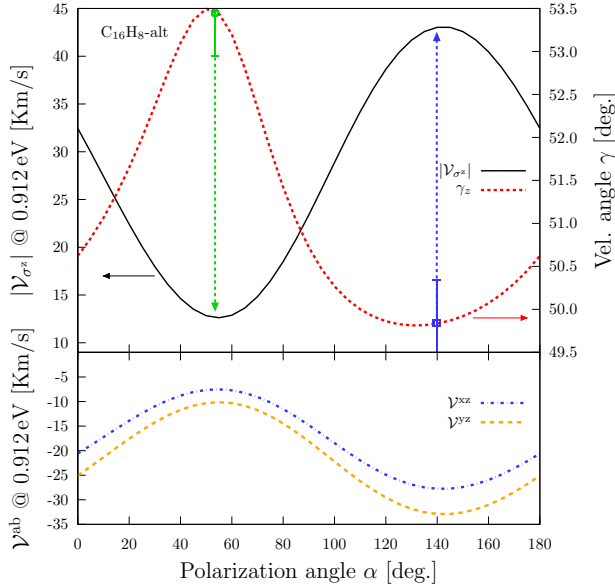
`fig:alt-3d-vsb`

FIG. 7. Most intense response of $|\mathcal{V}_{\sigma^z}|(\omega)$ (top frame, left scale) the corresponding velocity angle $\gamma_z(\omega)$ (top frame, right scale), the collinear (circled box) and perpendicular (square box) angles, and the two components $\mathcal{V}^{xz}(\omega)$ and $\mathcal{V}^{yz}(\omega)$ (bottom frame) for the *alt* structure fixing the energy to $0.912\,\mathrm{eV}$.

`fig:alt-vaz-rag`

tion angles α between $120°$ and $150°$. Also, a local maximum is obtained for the same polarization angles but for energies between $0.67\,\mathrm{eV}$ and $0.75\,\mathrm{eV}$. In the top frame of Fig. 7 we present in solid line the result of evaluate $|\mathcal{V}_{\sigma^z}|(\omega)$, related to the left scale, fixing the energy of the incoming beam to $0.912\,\mathrm{eV}$ for which value the response is maximized for the *alt* structure. In the same figure and frame we present in dashed line, related to the right scale, the velocity angle

$\gamma_z(\omega)$ and in the bottom frame the corresponding $\mathcal{V}^{xz}(\omega)$ and $\mathcal{V}^{yz}(\omega)$ components. Again, the circled and square boxes indicate the values for which the polarization angle and the velocity angle are parallel and perpendicular and with arrows are indicated the corresponding response value. From this figure and from Fig. 6 we have that the absolute maximum response for the *alt* structure is obtained for an incoming beam with polarization angle $\alpha = 145°$ reaching a velocity of $|\mathcal{V}_{\sigma^z}|(\omega) = 43.0\,\mathrm{Km/s}$ and for the spin polarized in the z direction and resulting in a velocity angle $\gamma_z(\omega) = 50°$ on the xy plane. The circled box for the collinear angle corresponds for angles α and $\gamma_z(\omega)$ equal to $53.5°$ with a value of $|\mathcal{V}_{\sigma^z}|(\omega) = 12.7\,\mathrm{Km/s}$, and the blue square box indicates the perpendicular angles for values $\alpha = 140°$ and $\gamma_z(\omega) = 50°$ with a value of $|\mathcal{V}_{\sigma^z}|(\omega) = 43\,\mathrm{Km/s}$. Finally we found that for variations of $\pm 0.5°$ of those collinear and perpendicular angles, presented with the error bars on the boxes, correspond ranges for the polarization angle $30° \leq \alpha \leq 70°$ and $95° \leq \alpha \leq 175°$ because the response angle $\gamma_z(\omega)$ has small variations for the complete range of the polarization angle α.

C. Fixing velocity

`sec:res-fixvel`

Up structure.

For the *up* structure we first analyzed the energy range from $0.00\,\mathrm{eV}$ to $0.16\,\mathrm{eV}$, where we found the most intense response and the absolute maxima for $|\mathcal{V}^x|(\omega)$ and $|\mathcal{V}^y|(\omega)$. In Fig. 8 we present the $|\mathcal{V}^a|(\omega)$ spectra resulting from evaluate the Eq. (8) using different polarization angles α in the Eq. (4) for the *up* structure. We can see that the onset of the response is when the energy of the incoming light is the same of the gap energy. From this picture we can see that for the zone between the energy range of $0.084\,\mathrm{eV}$-$0.093\,\mathrm{eV}$, corresponding to the THz radiation, and polarization angles between $30°$ and $45°$ is the zone where the maximum response is held for both, $|\mathcal{V}^x|(\omega)$ and $|\mathcal{V}^y|(\omega)$.

In the top frames of Figs. 9(a) and 9(b) we present in solid lines the results of $|\mathcal{V}^x|(\omega)$ and $|\mathcal{V}^y|(\omega)$, related to the left scale, fixing
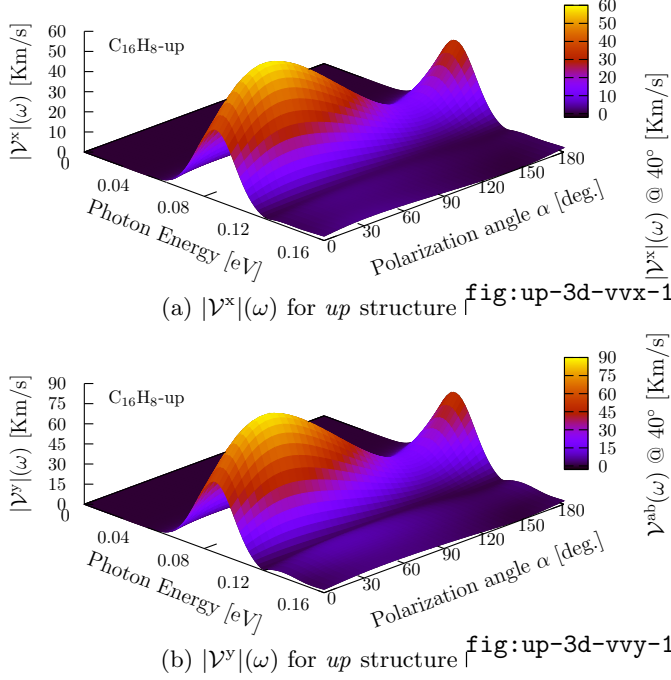
(a) $|\mathcal{V}^{\mathrm{x}}|(\omega)$ for *up* structure [`fig:up-3d-vvx-1`

(b) $|\mathcal{V}^{\mathrm{y}}|(\omega)$ for *up* structure [`fig:up-3d-vvy-1`

FIG. 8. $|\mathcal{V}^{\mathrm{a}}|(\omega)$ response vs. photon energy vs. polarization angle for the *up* structure. The absolute maxima of both responses $|\mathcal{V}^{\mathrm{x}}|(\omega)$ and $|\mathcal{V}^{\mathrm{y}}|(\omega)$ are localized in the energy range from $0.08\,\mathrm{eV}$ to $0.10\,\mathrm{eV}$ and for polarization angles from $25°$ to $50°$. `fig:up-3d-vva-1`

the polarization angle to $\alpha = 40°$ for which the response is maximized for the *up* structure. In the same figures and frames we present in dashed lines the corresponding polar $\theta_a(\omega)$ and azimuthal $\varphi_a(\omega)$ angles related to the right scale. Also, in the bottom frames of those figures we present the decomposition of $|\mathcal{V}^{\mathrm{x}}|(\omega)$ and $|\mathcal{V}^{\mathrm{y}}|(\omega)$ in the corresponding $\mathcal{V}^{\mathrm{xx}}(\omega)$, $\mathcal{V}^{\mathrm{xy}}(\omega)$, $\mathcal{V}^{\mathrm{xz}}(\omega)$, and $\mathcal{V}^{\mathrm{yx}}(\omega)$, $\mathcal{V}^{\mathrm{yy}}(\omega)$, $\mathcal{V}^{\mathrm{yz}}(\omega)$ components. From Fig. 9(a) we have that for an incoming bean with energy of $0.088\,\mathrm{eV}$ the three components have similar contributions and with values of $\mathcal{V}^{\mathrm{xx}}(\omega) = -36.5\,\mathrm{Km/s}$, $\mathcal{V}^{\mathrm{xy}}(\omega) = -23.2\,\mathrm{Km/s}$, and $\mathcal{V}^{\mathrm{xz}}(\omega) = 39.8\,\mathrm{Km/s}$ resulting in a value of $|\mathcal{V}^{\mathrm{x}}|(\omega) = 58.7\,\mathrm{Km/s}$ being this value the absolute maximum obtained when the spin-velocity is fixed in the x direction. To this value corresponds a polar and azimuthal angles of $\theta_{\mathrm{x}}(\omega) = 47$ and $\varphi_{\mathrm{x}}(\omega) = 212$, respectively, being directed upper the third Cartesian Quadrant of the xy plane. Also from this figure we have that those angle values are hold for almost all the peak of the response having a deviation of $\pm 2°$ in
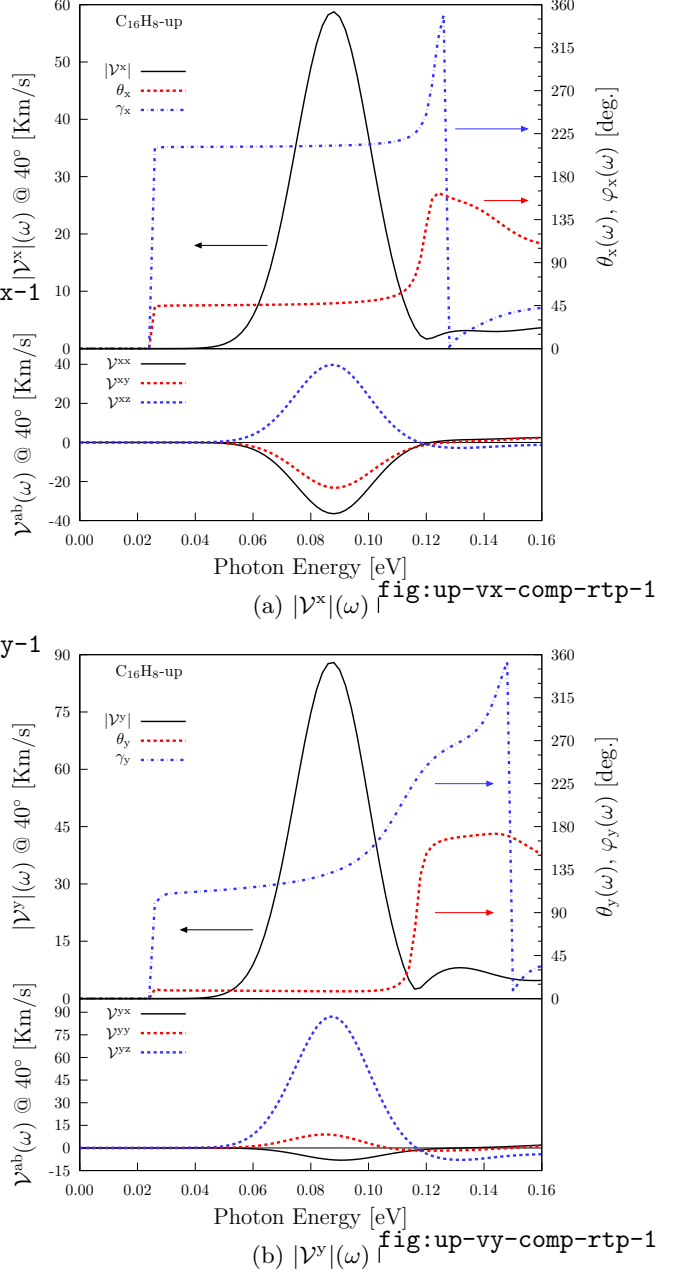

(a) $|\mathcal{V}^{\mathrm{x}}|(\omega)$ [`fig:up-vx-comp-rtp-1`

(b) $|\mathcal{V}^{\mathrm{y}}|(\omega)$ [`fig:up-vy-comp-rtp-1`

FIG. 9. Most intense response of $|\mathcal{V}^{\mathrm{x}}|(\omega)$ and $|\mathcal{V}^{\mathrm{y}}|(\omega)$ (top frames left scale of Figs. (a) and (b)), the corresponding polar φ and azimuthal θ angles (top frames right scale), and the corresponding three components (bottom frames) for the *up* structure fixing the polarization angle to $\alpha = 40°$ to maximize the response. `fig:up-vab-comp-rtp-1`

the range of energies from $0.028\,\mathrm{eV}$ to $0.098\,\mathrm{eV}$ from the corresponding to the absolute maximum mentioned before. Now, from Fig. 9(b) we have that the yx and yy components have less contributions for the total response than the yz and for the same incoming beam energy have val-
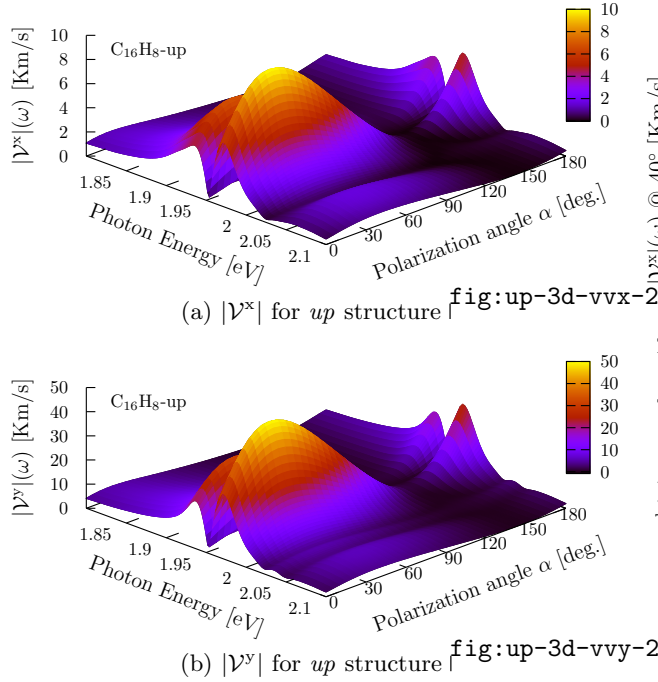
(a) $|\mathcal{V}^x|$ for *up* structure [`fig:up-3d-vvx-2`]

(b) $|\mathcal{V}^y|$ for *up* structure [`fig:up-3d-vvy-2`]

FIG. 10. $|\mathcal{V}^a|(\omega)$ response vs. photon energy vs. polarization angle for the *up* structure. The local maxima of both responses $|\mathcal{V}^x|(\omega)$ and $|\mathcal{V}^y|(\omega)$ are localized in the energy range from $1.95\,\text{eV}$ to $2.00\,\text{eV}$ and for polarization angles from $25°$ to $50°$. [`fig:up-3d-vva-2`]

ues of $\mathcal{V}^{yx}(\omega) = -7.9\,\text{Km/s}$ $\mathcal{V}^{yy}(\omega) = 8.6\,\text{Km/s}$, and $\mathcal{V}^{yz}(\omega) = 87.2\,\text{Km/s}$ resulting in a value of the total response of $|\mathcal{V}^y|(\omega) = 87.9\,\text{Km/s}$ being this value the absolute maximum obtained when the spin-velocity is fixed in the y direction and being 1.5 times more intense than $|\mathcal{V}^x|(\omega)$ To this absolute maximum correspond spin polar and azimuthal angles $\theta_y(\omega) = 8$ and $\varphi_y(\omega) = 133$, respectively, being directed almost perpendicularly over the xy plane and being localized on the first Cartesian Quadrant. In a different way than in the $|\mathcal{V}^x|(\omega)$ case only the polar angle is hold for the peak of the response having a deviation of $\pm 2°$ since the onset to a energy value of $0.106\,\text{eV}$ but the azimuthal angle changes since the onset to $0.106\,\text{eV}$ from $99°$ to $176°$. We also found that since the onset of the response till an energy for the incoming beam of $0.118\,\text{eV}$ the components of both, $|\mathcal{V}^x|(\omega)$ and $|\mathcal{V}^y|(\omega)$ have no change in the spin polarization direction. Finally, after this energy value both goes to zero. Also there is another energy range of interest for an incoming energy beam from $1.80\,\text{eV}$ to
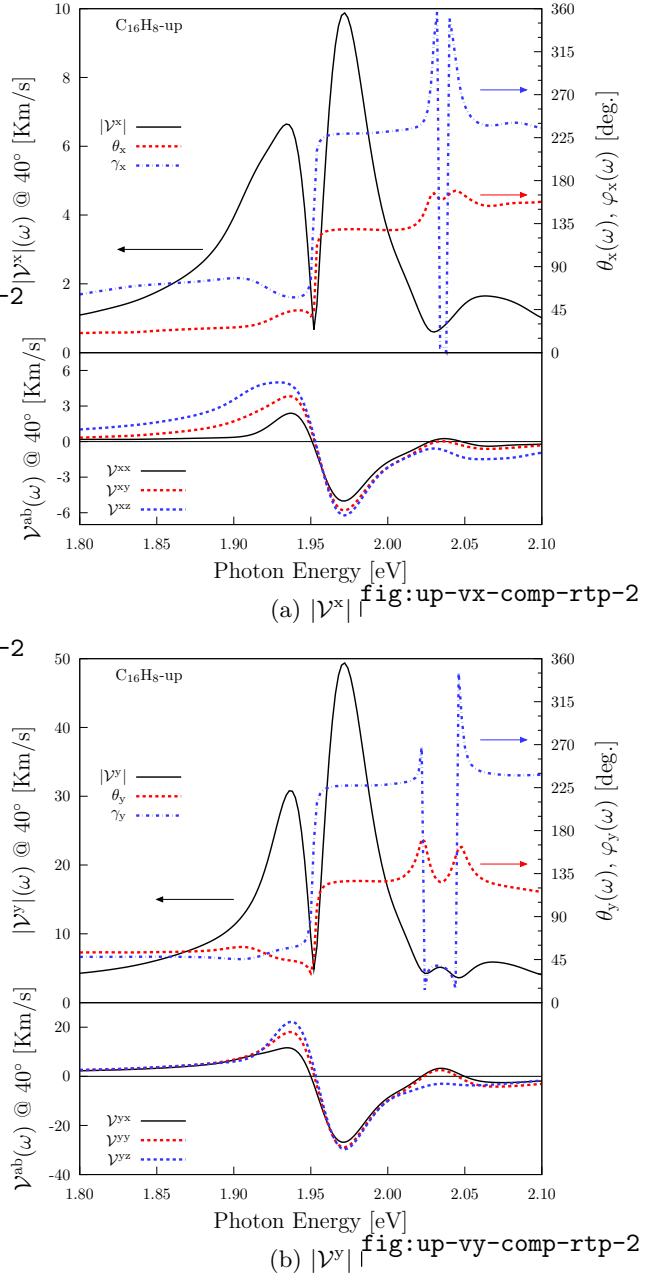

(a) $|\mathcal{V}^x|$ [`fig:up-vx-comp-rtp-2`]

(b) $|\mathcal{V}^y|$ [`fig:up-vy-comp-rtp-2`]

FIG. 11. Intense response of $|\mathcal{V}^x|(\omega)$ and $|\mathcal{V}^y|(\omega)$ (top frames left scale of Figs. (a) and (b)), the corresponding polar φ and azimuthal θ angles (top frames right scale), and the corresponding three components (bottom frames) for the *up* structure fixing the polarization angle to $\alpha = 40°$ to maximize the response. [`fig:up-vab-comp-rtp-2`]

$2.10\,\text{eV}$, corresponding to the THz and visible radiation, presented in Fig. 10 where two local maxima of $|\mathcal{V}^x|(\omega)$ and $|\mathcal{V}^y|(\omega)$ are obtained for the *up* structure. From this figure we have that for the zone between the energy ranges from $1.92\,\text{eV}$ to $1.94\,\text{eV}$ and from $1.96\,\text{eV}$ to $1.98\,\text{eV}$

and for polarization angles from $30°$ to $45°$ those two local maxima zones are held. We found that the two local maxima are obtained for an energy of the incident beam energies of 1.934 eV and 1.972 eV fixing again the polarization angle to $40°$. In the top frames of Figs. 11(a) and 11(b) we present in solid lines the results of $|\mathcal{V}^x|(\omega)$ and $|\mathcal{V}^y|(\omega)$, related to the left scale, fixing the polarization angle to $\alpha = 40°$ for which the response is maximized for the *up* structure. In the same figures and frames we present in dashed lines the corresponding polar ($\theta_x(\omega)$ and $\theta_y(\omega)$) and azimuthal ($\varphi_x(\omega)$ and $\varphi_y(\omega)$) angles related to the right scale. In the bottom frames of same figures we present the decomposition of the responses in the three corresponding components $\mathcal{V}^{xx}(\omega)$, $\mathcal{V}^{xy}(\omega)$, $\mathcal{V}^{xz}(\omega)$ and $\mathcal{V}^{yx}(\omega)$, $\mathcal{V}^{yy}(\omega)$, $\mathcal{V}^{yz}(\omega)$. We found that for both cases, the components have similar contributions and for an incoming energy beam of 1.934 eV we have the first local maximum resulting in a value of $|\mathcal{V}^x|(\omega) = 6.6$ Km/s along the x direction with polar and azimuthal spin polarization angles $\theta_x(\omega) = 42°$ and $\varphi_x(\omega) = 59°$ having fluctuations but being directed over the first Cartesian Quadrant of the xy plane. For the spin moving along the y direction we have a value of $|\mathcal{V}^y|(\omega) = 28.7$ Km/s with polar and azimuthal angles $\theta_y(\omega) = 45°$ and $\varphi_y(\omega) = 56°$ having variations of $\pm 5°$ for energy variations of ± 0.01 eV and being directed over the fir Cartesian Quadrant of the xy plane. Alike, for an incoming energy beam of 1.972 eV we found the second and more intense local maxima with all the components of both responses having similar contributions and resulting in values of $|\mathcal{V}^x|(\omega) = 9.9$ Km/s and spin polarization angles $\theta_x(\omega) = 129°$ and $\varphi_x(\omega) = 229°$ being almost constant in the width of the peak having variations of $\pm 1°$ for variations in energy of ± 0.01 eV and being directed downward the third Cartesian Quadrant of the xy plane. For the spin moving in the y direction we have a value of $|\mathcal{V}^y|(\omega) = 49.4$ Km/s with spin polarization angles $\theta_y(\omega) = 127°$ and $\varphi_y(\omega) = 227°$ being almost constant with variations of $\pm 1°$ for variations in energy of ± 1 eV and being directed downward the third Cartesian Quadrant of the xy plane. Finally we have that for bot energies $|\mathcal{V}^y|(\omega)$ is more intense than $|\mathcal{V}^x|(\omega)$

(a) $|\mathcal{V}^x|$ for *alt* structure [`fig:alt-3d-vvx`

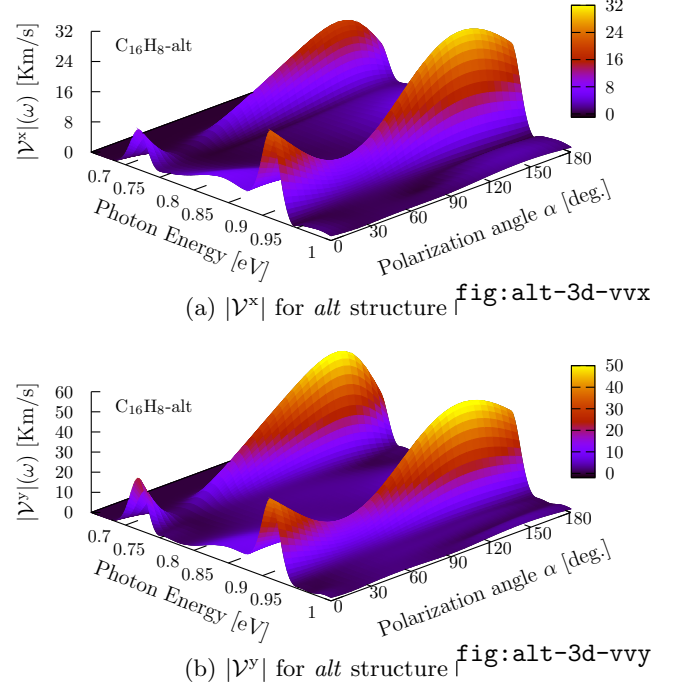(b) $|\mathcal{V}^y|$ for *alt* structure [`fig:alt-3d-vvy`

FIG. 12. $|\mathcal{V}^a|(\omega)$ response vs. photon energy vs. polarization angle for the *alt* structure. The absolute maxima of both responses $|\mathcal{V}^x|(\omega)$ and $|\mathcal{V}^y|(\omega)$ are localized in the energy range from 0.90 eV to 0.93 eV and for polarization angles from $120°$ to $150°$. `fig:alt-3d-vva`

being 4.4 times more intense for 1.932 eV and 5.0 times more intense for 1.972 eV. Also all the components of the responses keep the spin polarization positive till an energy of the incoming beam equal to 1.954 eV when the spin polarization changes the direction and after an energy for the incoming beam equal to 2.05 eV both responses goes to zero.

Alt structure.

For the *alt* structure we analyzed the energy range from 0.6 eV to 1.0 eV, corresponding to the THz radiation, where we found the a local maxima and the most intense responses for $|\mathcal{V}^x|(\omega)$ and $|\mathcal{V}^a|(\omega)$. In Fig. 12 we present the $|\mathcal{V}^a|(\omega)$ spectra resulting from evaluate again Eq. (8) using different polarization angles α in Eq. (4) but now for the *alt* structure. We can see that the onset of the response is when the energy of the incoming light is the same of the gap energy. From this picture we can see that for the zone between the energy range of 0.90 eV-0.93 eV and polarization angles between $120°$ and $150°$ is the zone where the maximum response for both,
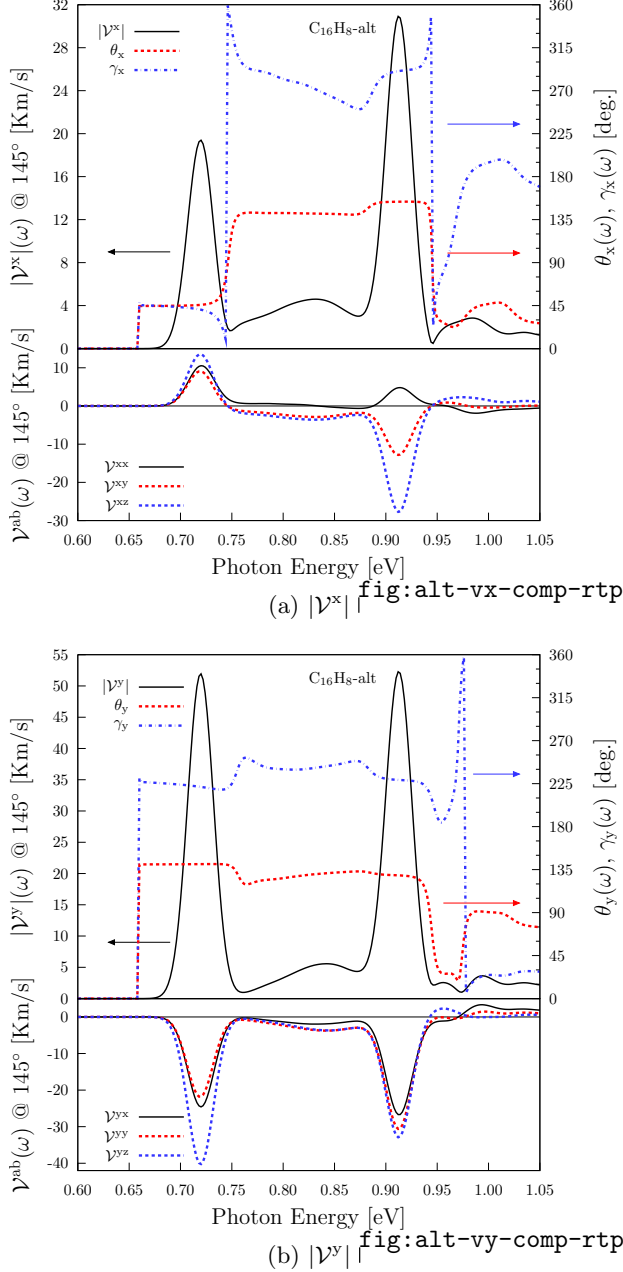
(a) $|\mathcal{V}^{\mathrm{x}}|$ `fig:alt-vx-comp-rtp`

(b) $|\mathcal{V}^{\mathrm{y}}|$ `fig:alt-vy-comp-rtp`

FIG. 13. Most intense response of $|\mathcal{V}^{\mathrm{x}}|(\omega)$ and $|\mathcal{V}^{\mathrm{y}}|(\omega)$ (top frames left scale of Figs. (a) and (b)), the corresponding polar φ and azimuthal θ angles (top frames right scale), and the corresponding three components (bottom frames) for the *alt* structure fixing the polarization angle to $\alpha = 145°$ to maximize the response.

`fig:alt-vab-comp-rtp`

$|\mathcal{V}^{\mathrm{x}}|(\omega)$ and $|\mathcal{V}^{\mathrm{y}}|(\omega)$ is held. We also found that the first peak is obtained when the energy of the incoming beam is $0.720\,\mathrm{eV}$ and the absolute maximum of the response is obtained when for $0.912\,\mathrm{eV}$, both for a polarization angle $\alpha = 145°$.

In the top frames of Figs. 13(a) and 13(b) we present in solid lines the results of $|\mathcal{V}^{\mathrm{x}}|(\omega)$ and $|\mathcal{V}^{\mathrm{y}}|(\omega)$, related to the left scale, fixing the polarization angle to $\alpha = 145°$ for which the response is maximized for the *alt* structure. In the same figures and frames we present ind dashed lines the spin polarization angles related to the right scale and in the bottom frames the corresponding three components. Making the analysis for the components and angles when the spin current is directed in the x direction, corresponding to the Fig. 13(a), we found that for the *alt* structure when the energy of the incoming beam is $0.720\,\mathrm{eV}$ we have similar contributions from all the components resulting in a response of $|\mathcal{V}^{\mathrm{x}}|(\omega) = 19.4\,\mathrm{Km/s}$ and polar and azimuthal spin polarization angles $\theta_{\mathrm{x}}(\omega) = 46°$ and $\varphi_{\mathrm{x}}(\omega) = 41°$ having variations in the range of the peak but being directed over the first Cartesian Quadrant of the xy plane; for an energy of $0.912\,\mathrm{eV}$ we have a major contribution from the $\mathcal{V}^{\mathrm{xz}}(\omega)$ component resulting in a total response of $|\mathcal{V}^{\mathrm{x}}|(\omega) = 30.9\,\mathrm{Km/s}$ and angles $\theta_{\mathrm{x}}(\omega) = 154°$, and $\varphi_{\mathrm{x}}(\omega) = 290°$ having variations of $\pm3°$ in for energy variations of $\pm1\,\mathrm{eV}$ and being directed downward the fourth Cartesian Quadrant of the xy plane. Making now the analysis for the components and angles when the spin current is directed along the y direction, corresponding to the Fig. 13(b), we found that when the energy of the incoming beam is $0.720\,\mathrm{eV}$ we have more contribution from the $\mathcal{V}^{\mathrm{yz}}(\omega)$ component resulting in a response of $|\mathcal{V}^{\mathrm{y}}|(\omega) = 51.9\,\mathrm{Km/s}$ and angles $\theta_{\mathrm{y}}(\omega) = 141°$ and $\varphi_{\mathrm{y}}(\omega) = 222°$ being the first constant and the second having variations of $\pm3°$ for energy variations of $\pm0.3\,\mathrm{eV}$ and being directed downward the third Cartesian Quadrant of the xy plane. Then, for the peak centered at $0.912\,\mathrm{eV}$ we have similar contributions of all the components resulting in a response $|\mathcal{V}^{\mathrm{y}}|(\omega) = 52.3\,\mathrm{Km/s}$ being this the absolute maximum response for the *alt* structure. The corresponding angles are $\theta_{\mathrm{y}}(\omega) = 129°$ and $\varphi_{\mathrm{y}}(\omega) = 229°$ being both constant for the energy range of the peak and being directed downward the third Cartesian Quadrant of the xy plane. Finally we have that the three components of $|\mathcal{V}^{\mathrm{y}}|$ are negative keeping the same spin polarization since the onset of the response to a en-
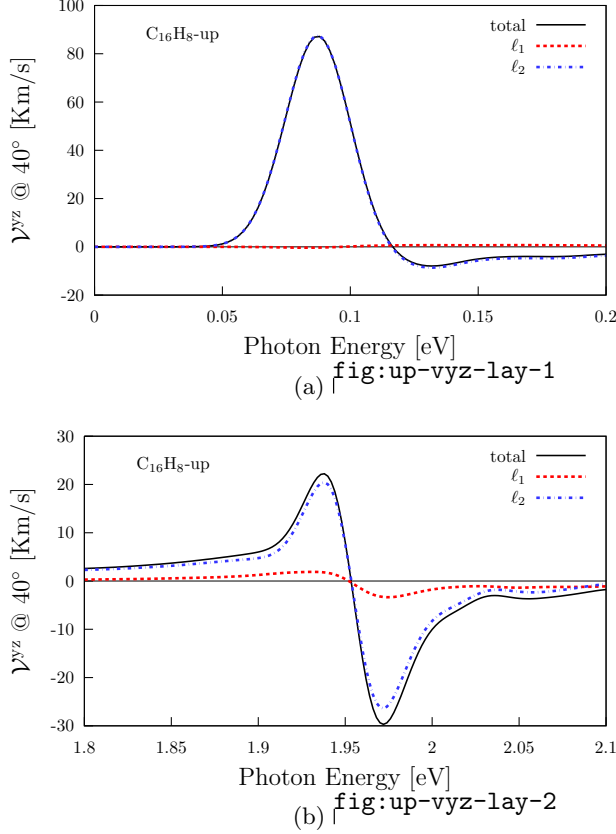
(a) | fig:up-vyz-lay-1

(b) | fig:up-vyz-lay-2

FIG. 14. Layer-by-layer contribution of $\mathcal{V}^{yz}$ for the *up* structure.

fig:up-vyz-lay

ergy of the incoming beam of 0.886 eV when the response decreases and goes to zero.

IV. LAYER-BY-LAYER ANALYSIS

sec:res-layer_by_layer_analysis

The structures presented here where divided into layers to analyze the he layer-by-layer contribution for $\mathcal{V}^{ab}$ response. The *alt* structure was divided in six layers corresponding the first one to the top hydrogen atoms, from the second to the forth to carbon atoms in different z positions, and the sixth and last one to the bottom hydrogen atoms. The *up* structure was divided into two layers, the first one comprised by the top hydrogen atoms and the second by the carbon atoms. The layer divisions and atom positions for the unit cells are shown in Tables I and II.

From the bottom frames of Figs. 9 and 11 we can see that for the *up* structure again the most

intense component of $|\mathcal{V}^x|$ and $|\mathcal{V}^y|$ corresponds to $\mathcal{V}^{yz}$ which has a value of 87.2 Km/s for an energy incident beam of 0.088 eV and -29.7 Km/s for an energy incident beam of 1.972 eV. This component and the corresponding layer by layer contribution is depicted in Fig. 14s. From this figure we have that for the energy range from 0 eV to 0.2 eV the response comes from the second layer composed by carbon atoms presented in Tab. II and denoted by the number 2 in Fig. 2. In the other hand, the response for the energy range from 1.8 eV to 2.1 eV almost all the response comes from the carbon atoms having a leaser contribution from the hydrogen layer. From the bottom frames of Fig. 13 we can see that for the *alt* structure the most intense component of $|\mathcal{V}^x|$ and $|\mathcal{V}^y|$ corresponds to $\mathcal{V}^{yz}$ which has a value of -40.2 Km/s for an energy incident beam of 0.72 eV. This component and the corresponding layer by layer contribution is depicted in Fig. 15. From this figure we have that for the energy range from 0.70 eV to 0.74 eV the fifth and sixth layers corresponding to the bottom carbon and hydrogen numbered with 5 and 6 in Fig. 1 have contributions in opposite direction than the other 4 layers resulting in a total response $\mathcal{V}^{yz} = -40.2$ Km/s for an incoming beam energy of 0.72 eV. In the other hand, for the energy range from 0.88 eV to 0.95 eV the response for the all six layers the responses are in the same direction resulting in a total response $\mathcal{V}^{yz} = -32.89$ Km/s for an incoming beam with energy of 0.912 eV.
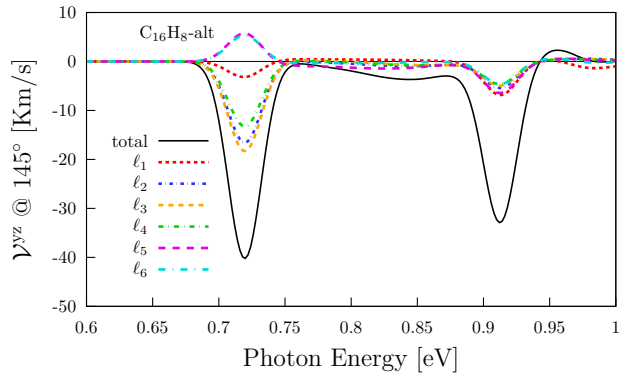

FIG. 15. Layer-by-layer contribution of $\mathcal{V}^{yz}$ for the *alt* structure.

fig:alt-vyz-lay

[1] N. Arzate, R. A. Vázquez-Nava, and B. S. Mendoza, Phys. Rev. B **90**, 205310 (2014).

[2] X. Gonze, B. Amadon, P.-M. Anglade, J.-M. Beuken, F. Bottin, P. Boulanger, F. Bruneval, D. Caliste, R. Caracas, M. Côté, T. Deutsch, L. Genovese, P. Ghosez, M. Giantomassi, S. Goedecker, D. Hamann, P. Hermet, F. Jollet, G. Jomard, S. Leroux, M. Mancini, S. Mazevet, M. Oliveira, G. Onida, Y. Pouillon, T. Rangel, G.- M. Rignanese, D. Sangalli, R. Shaltaf, M. Torrent, M. Verstraete, G. Zerah, and J. Zwanziger, Comput. Phys. Commun. **180**, 2582 (2009).

[3] C. Hartwigsen, S. Goedecker, and J. Hutter, Phys. Rev. B **58**, 3641 (1998).

[4] G. Onida, L. Reining, and A. Rubio, Rev. Mod. Phys. **74**, 601 (2002).LastBibItem